

## Top quark physics in ATLAS

---

**Krzysztof Sliwa\***

*Tufts University*

*E-mail:* [krzysztof.sliwa@tufts.edu](mailto:krzysztof.sliwa@tufts.edu)

A review of top quark physics and results from the ATLAS Collaboration is presented. Most of the results[1] are based on the data from the LHC Run 1, in which the ATLAS detector recorded events from proton-proton collisions corresponding to the integrated luminosity of  $\sim 5/fb$  at  $\sqrt{s} = 7 TeV$  and  $\sim 20/fb$  at  $\sqrt{s} = 8 TeV$ .

*Proceedings of the Corfu Summer Institute 2015 "School and Workshops on Elementary Particle Physics and Gravity"*

*1-27 September 2015*

*Corfu, Greece*

---

\*Speaker.

## 1. The Standard Model and beyond

The Standard Model (SM) of particle physics[2], developed in 1961-1972, is a gauge theory based on the  $SU(3)_C \times SU(2)_I \times U(1)_Y$  symmetry group (C-colour, I-weak isospin and Y-hypercharge). The  $SU(3)_C$  is an unbroken symmetry, it is the basis of Quantum Chromo-Dynamics (QCD), a quantum theory of strong interactions, whose carriers, massless gluons, couple to color (strong force charge). The  $SU(2) \times U(1)$  - which gives rise to the quantum theory of electroweak interactions - is spontaneously broken by the Brout-Englert-Higgs mechanism, which gives mass to the electroweak bosons (massive  $W^+$ ,  $W^-$ ,  $Z^0$  and a massless photon), and all fermions.

Matter is build of fermions - quarks and leptons. There are three families of each, with corresponding antiparticles. Quarks exist in three colors, leptons are color singlets, and as such they do not couple to gluons, and they don't interact strongly. Bosons are the carriers of interactions: there are 8 massless gluons, three heavy weak bosons ( $W^\pm, Z^0$ ) and a massless photon. In the Minimal Standard Model (MSM), the Higgs sector is the simplest possible, it contains a single weak isospin doublet of complex Higgs fields, which after giving masses to  $W^+$ ,  $W^-$ ,  $Z^0$ , leaves a single neutral scalar Higgs particle. A neutral scalar Higgs field permeates the Universe and is, in some way, responsible for masses of other particles - they originate from couplings to the Higgs field. There are 26 parameters not predicted by MSM - masses of quarks and leptons, coupling constants, Higgs mass and the vacuum expectation value, mixing angles and complex phases in the quark Cabibbo-Kobayashi-Maskawa mixing matrix and the lepton Maki-Nakagawa-Sakata mixing matrix, and the QCD phase,  $\theta$ . All must be measured.

The discovery of the Higgs boson, the only particle missing in the MSM, was announced on July 4th, 2012 by the ATLAS and CMS Collaborations at the Large Hadron Collider (LHC) at CERN. It was a great success for those more than 20 years-long projects. The discovery also brought many questions, some new and many old, the most important one: is the new particle the Minimal Standard Model boson? Answering this question will take time and many precision measurements. With the Higgs mass known, all MSM couplings can be calculated. There are many outstanding questions in the SM: why so many (26) free parameters: all masses, all couplings, all mixing angles and CP-violating phases; why 6 quarks and 6 leptons - is there an additional symmetry? why quarks and leptons come in three pairs (generations)? is CP not an exact symmetry, or why are laws of physics not symmetrical between matter and antimatter - is this fact related to the questions of why is our Universe matter-dominated? there seem to be not enough sources of CP violation in the SM to explain the latter? what is the nature of Dark Matter, about 5 times more prevalent in the Universe than ordinary matter? how to include gravity ? There is still plenty to understand, and all this means that the Standard Model is perhaps just a low energy approximation.

Many new theories were considered as possible beyond Standard Model physics models: Supersymmetry (SUSY); Grand Unified Theories based on some larger symmetry groups, e.g. SU(5), SO(10), E8, Monster group... There exist also "new physics" models based on the extensions of Kaluza-Klein theory, string theory, superstring theory, branes, M-theory, quantum gravity or Technicolor. Finding Higgs boson does not solve SM shortcomings. It is quite clear that new experimental data and analyses are badly needed. (Personally, I think it would be much more interesting if the Higgs boson were not there, or if the new-found particle is *NOT* a Minimal Standard Model

boson).

## 2. Top Quark in the Standard Model

The top quark was expected in the Standard Model (SM) of electroweak interactions as a partner of the b-quark in a SU(2) doublet of weak isospin in the third family of quarks. The first evidence for top quark was published by CDF in 1994[3], after some earlier hints, and was followed by the discovery papers by CDF and D0 Collaborations in 1995[4]. Top quark mass is about 173 GeV, which makes the top quark the most massive of the known elementary particles, and it may be playing a special role in electroweak symmetry breaking.

At the LHC, achieving a good understanding of top physics is a necessary first step in almost any search for physics beyond the Standard Model at high mass scale. Most “new physics ”will show up as excess of events beyond the SM expectations, including 6 quarks. Top quark production will be the most dominant background in almost any new physics searches, and has to be understood well.

In addition to direct searches for “new physics ”, the precision studies of  $t\bar{t}$  spin correlations and asymmetries could be one of the best window to the “beyond the SM ”physics. Top studies may also be the best testing ground for the higher order theoretical calculations. Recently, significant progress has been achieved with Czakon and Mitov finalizing the complete NNLO calculations[5].

Studies of top quarks are very interesting on their own. Because of very large mass of the top quark, its lifetime is very short,  $\sim 5 \times 10^{-25}$  seconds, much shorter than the characteristic time of the strong interactions, which is of the order of  $\sim 10^{-22}$  seconds. Top quark thus decays before any effects due to the strong interactions (hadronization) may take place. This allows a direct access to the information about the top quark spin, which is very difficult, if not impossible, for any other quark.

## 3. ATLAS at the LHC

The LHC proton-proton accelerator was approved by CERN Council in 1994. The construction started after closing of LEP2 in 2000, and the first long physics run started on March 30, 2010, when the first collisions at  $\sqrt{s} = 7 \text{ TeV}$  were recorded. In May 2012, the energy of pp collisions was increased to 8 TeV. In the first physics run of the LHC, each of the two large LHC detectors, CMS and ATLAS, recorded data corresponding to the luminosities of 5/fb at 7 TeV and 20/fb at 8 TeV. After a technical shutdown in which major upgrades to the LHC were performed, the LHC Run 2 started in May 2015, with first stable beam collisions at pp energy of  $\sqrt{s} = 13 \text{ TeV}$ . The ATLAS detector has been described in details elsewhere[6]. It is a multi-purpose particle physics detector, forward-backward symmetric and with cylindrical geometry. The inner tracking detectors are surrounded by a thin superconducting solenoid magnet, electromagnetic and hadronic calorimeters, and a muon spectrometer with an axial magnetic field generated by three superconducting toroidal magnets, each with eight coils. The inner tracker (ID), in combination with the 2T magnetic field from the solenoid, provides precision momentum measurements for charged particle within the pseudorapidity range  $|\eta| < 2.5$ . It consists of, moving from the interaction point to the

outside, a silicon pixel detector, a silicon microstrip detector and a straw-tube tracker that also provides transition radiation measurements for electron identification. The calorimeter system covers the pseudorapidity range  $|\eta| < 4.9$ . A high-granularity liquid-argon (LAr) sampling calorimeter with lead absorber provides the measurement of the electromagnetic showers (EM) within  $|\eta| < 3.2$ . In the region matched to the ID,  $|\eta| < 2.5$ , the innermost layer has a fine segmentation in  $\eta$  to allow  $e/\gamma$  separation from  $\pi^0$  and to improve the resolution of the shower position and direction measurements. Hadronic showers (HAD) are measured by an iron/plastic scintillator tile calorimeter in the central region,  $|\eta| < 1.7$ , and by a LAr calorimeter in the end-cap region,  $1.5 < |\eta| < 3.2$ . In the forward region, measurements of both EM and HAD are provided by a LAr calorimeter covering the pseudorapidity range  $3.1 < |\eta| < 4.9$ . The muon spectrometer (MS), with its own trigger and high precision tracking detectors, provides muon identification for charged tracks within  $|\eta| < 2.7$ . The combination of all ATLAS detector systems provides charged particle measurements, and lepton and photon measurements and identification in the pseudorapidity range  $|\eta| < 2.5$ . Jets and missing transverse energy,  $\cancel{E}_t$ , are reconstructed over the full range covered by the calorimeters,  $|\eta| < 4.9$ .

The LHC is a true top factory. The cross sections for the top pair and single top production, and the number of expected events, shown in Figure 1, are many orders of magnitude higher than at Tevatron.

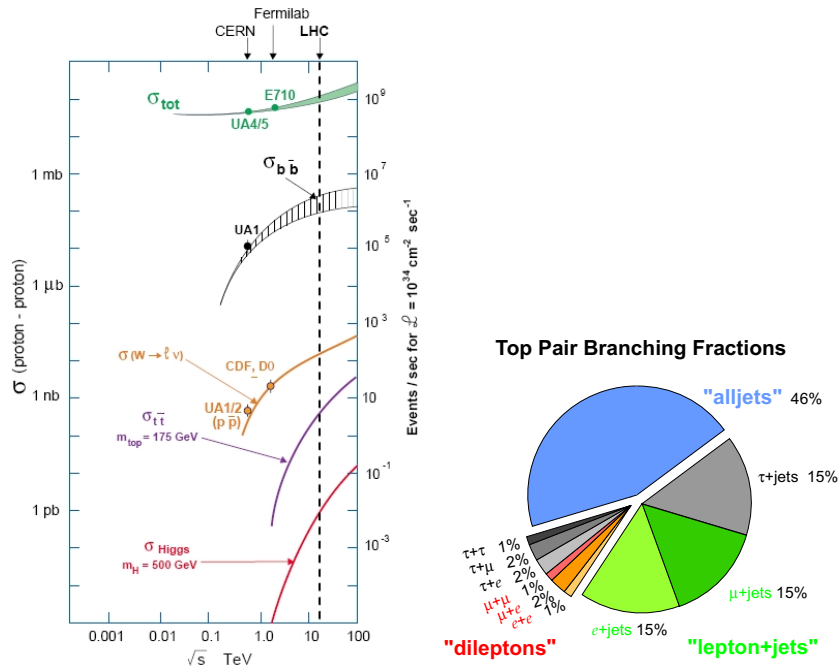


**Figure 1:** Left: Cross sections for selected processes at the Tevatron and the LHC. Right: Final states in top pair ( $t\bar{t}$ ) production

#### 4. Methodology of top measurements and studies

Top studies, in addition to provide measurements of its properties, they also provided a testing

ground for many novel analysis techniques. At the Tevatron at FNAL, the samples of top events were small and advanced methods were necessary to extract best results. At the LHC at CERN, statistics is not a problem, however, the use of clever analysis techniques leads to smaller errors. Among the techniques used are: i) kinematic fitting; ii) template fitting (single or multidimensional); iii) various "matrix element" techniques; iv) machine learning techniques - neural networks (NN), boosted decision trees (BDT) and support vector machines (SVM).

In the SM, top quarks decay predominantly into a  $W$  boson and a  $b$ -quark,  $t \rightarrow W^+b, \bar{t} \rightarrow W^- \bar{b}$ . The top pair production candidates are usually classified into of the three final final state topologies: i) dileptons - events in which both  $W$  bosons decay leptonically, such events have the smallest backgrounds, especially in the  $e\mu$  channel; ii) lepton+jets - these events have larger branching fractions but also larger backgrounds:  $W$ +jets,  $Z$ +jets, lepton fakes; iii) "all hadronic" - most abundant but with the largest backgrounds. The top pair branching fractions are shown in Figure 1. Identifying a  $b$ -quark in the final state is also an important element in top analyses. Specialized high-resolution tracking detectors look for a displaced vertex from a decay of relatively long-lived particles containing  $b$ -quark from top quark decay, and "soft" lepton tagging algorithms look for additional leptons within jets, expected in jets originating from  $b$ -quarks. Usually a combination of several tagging techniques is used. ATLAS uses a neural net algorithm, MV1, to combine results from several algorithms, operating with the tagging efficiency of  $\sim 70\%$ .

#### 4.1 Cross section

The measurement of the cross section is one of the simplest one can perform. The steps are, for both the  $t\bar{t}$  and the single top production measurements:

- search for events with top signature
- calculate the expected SM background
- count events above backgrounds
- apply corrections for acceptance and reconstruction inefficiencies and biases

One should remember two important facts:

- i) It is assumed that the selected events contain just the  $t\bar{t}$  events and the SM background. This is the simplest and the most natural hypothesis since top quark is expected in the SM.
- ii) Some of the acceptance corrections are strongly varying functions of the top quark mass,  $M_{top}$ . The measured cross section depends on the adopted value of  $M_{top}$ , which has to be determined independently.

#### 4.2 Direct measurement of the top quark mass

All techniques assume that each of the selected event contains a pair of massive objects of the same mass ( $t$  and  $\bar{t}$  quarks), which subsequently decay as predicted in SM. A variety of fitting techniques have been developed which use information about the event kinematics. In addition to the assumption mentioned in the previous section, there is also an important question about the meaning of the measured parameter - what is really measured: "Pythia" mass, MS mass, pole mass?

In the lepton+jets and all-hadronic final states there are enough kinematical constraints to perform a genuine fit (3C or better in the language of kinematical fitters). A one-to-one mapping between the observed leptons and jets and the fitted partons is assumed. Leptons are measured best, jets not as well, while the missing transverse energy,  $\cancel{E}_t$ , has the largest uncertainty. In the lepton+jets final state one may, or may not, use  $\cancel{E}_t$  as the starting point for the transverse energy of the missing neutrino. Most analyses they make use of MET. ATLAS and CMS use a number of methods: template, multivariate template, DLM, ideogram, and multivariate discriminant (NN, BDT) analyses to select their top enriched and background samples of events that are basis of their top mass and cross section analyses. Even if only 4 highest transverse energy jets are used, there are 12 combinations if no tagging requirement is used; 6 combinations with one tagged jet, and two when one requires two tagged jets. One should remember that quite often additional jets due to the initial and final state radiation (ISR and FSR) are present in an event. The best measurements of the top quark mass are obtained by calculating the mass of the three jets originating from the hadronic decay of a top quark, using lepton as a trigger, and simultaneously correcting the jet energies by implementing a  $W$  mass constraint for the non-tagged jets in the three jet system of the hadronically decaying top quark.

In the di-lepton mode situation is much more complicated, as the problem is underconstrained - there are two missing neutrinos in each event!. Several techniques were developed. All obtain a probability density distribution as a function of top quark mass, whose shape allows identifying the most likely mass which satisfies the hypothesis that a pair of top quarks were produced in an event and that their decay products correspond to a given combination of leptons and jets.  $\cancel{E}_t$  may, or may not, be used. Experimenters developed several methods, for example: the Neutrino Phase Space weighting technique, the Average Matrix Element technique (MWT), Dalitz-Goldstein and Kondo "matrix element" methods, "Minit" fitting. Most techniques use the missing transverse energy  $\cancel{E}_t$ , but not all - the modified Dalitz-Goldstein method includes instead - in the definition of the likelihood, in a Bayesian way - information about the parton distribution functions, transverse energy of the  $t\bar{t}$  system and the angular correlations between the top decay products.

## 5. ATLAS results

### 5.1 Top-antitop quark pair production

The leading order (LO) Feynman diagrams for the production of a top-antitop pair via the strong and electroweak interactions are shown in Figure 2. A summary of the ATLAS (and CMS) top pair cross section measurements at  $\sqrt{s} = 7 \text{ TeV}$  and  $8 \text{ TeV}$  are shown in Figure 3. The preliminary measurement of the top pair cross section in the dilepton  $e\mu$  with tagged b-quark jets final state, in which the background is very small, is shown in Figure 4. The measured values of the top pair production cross sections at  $7 \text{ TeV}$ ,  $8 \text{ TeV}$  and  $13 \text{ TeV}$  are compared with the NNLO calculations[5], with very good agreement.

### 5.2 Single top quark production

The tree level (LO) diagrams of single top quark production processes ( $t$ -channel,  $Wt$ -channel and  $s$ -channel) are shown in Figure 5. The corresponding measurements of the cross sections (only

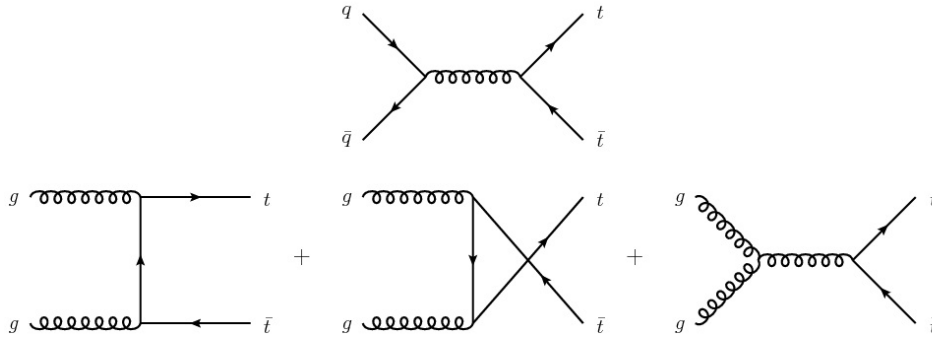


**Figure 2:** Tree level diagram for the  $t\bar{t}$  production in the MSM via strong interactions.

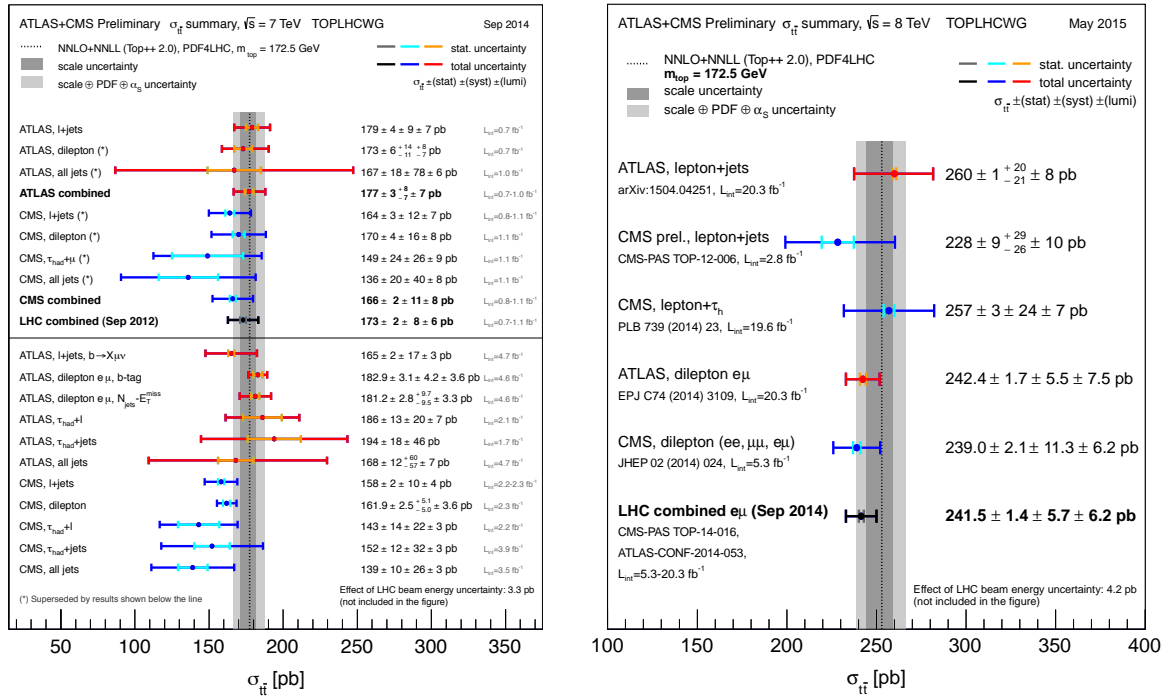


**Figure 3:** A summary of the ATLAS and CMS top pair cross section measurements at 7 TeV and 8 TeV. Also shown are the LHC combinations of the respective results. References to the original publications are listed in the Figure.

limits for the s-channel) from ATLAS, CMS and the LHC combinations are shown in Figures 6. The measurements of the single top production rate provide a direct access to the  $Wtb$  vertex, and allow determination of the  $|V_{tb}|$  element of the Cabibbo-Kobayashi-Maskawa matrix. The results of such analyses are also shown in Figure 6, on the right side.

### 5.3 Top quark mass

The direct measurements of the top quark mass by ATLAS, CMS and the LHC combination are summarized in Figure 7. An indirect measurement of the top pole mass, obtained from comparing

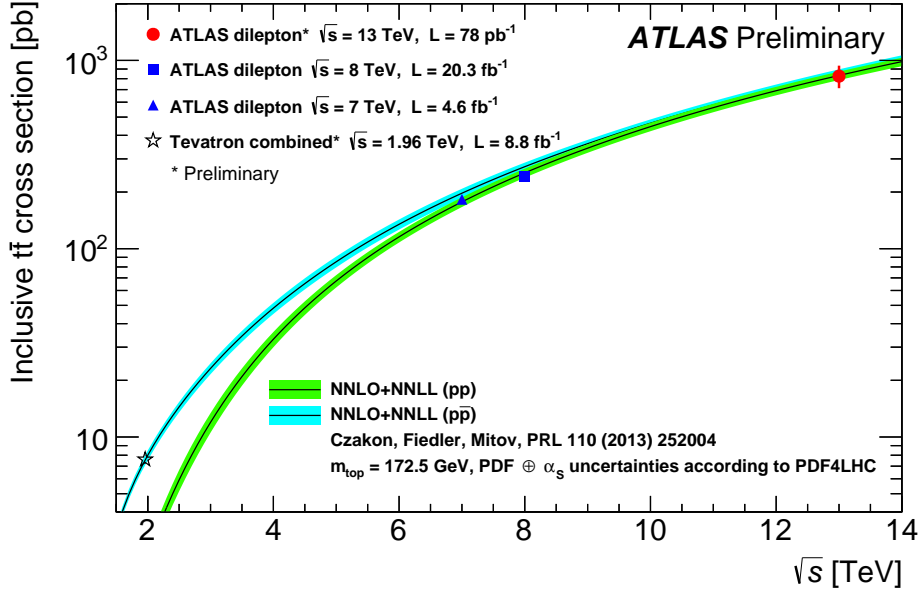


**Figure 4:** The cross section measurements by the ATLAS collaboration at  $pp$  collisions at the LHC at 7 TeV, 8 TeV and 13 TeV, and at  $p\bar{p}$  collisions at the Tevatron at 1.96 TeV, compared with the NNLO calculations.

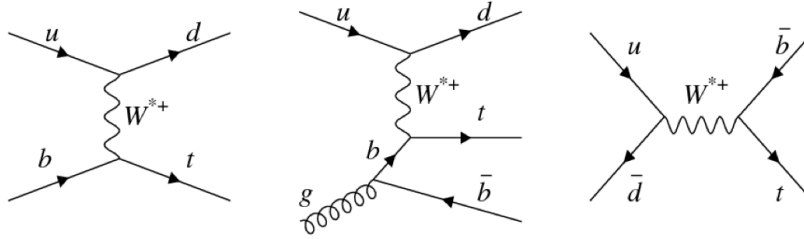


**Figure 5:** The tree level diagrams for single top production in the MSM. From the left:  $t$ -channel,  $Wt$ -channel,  $s$ -channel.

the differential cross section of  $t\bar{t} + 1$  jet events with the NLO calculation[7], obtained with the ATLAS 7 TeV data[8] yields  $173.7^{+2.3}_{-2.1}$  GeV.

## 6. Top spin polarization and correlations

The top quark decays via the weak interactions, predominantly into a  $W$  boson and a  $b$ -quark. Because of the very large mass of the top quark, its lifetime is very short,  $\sim 5 \times 10^{-25}$  seconds, much shorter than the characteristic time of the strong interactions. The top quark decay products will not be altered by the strong interactions, which is unique among all quarks. This gives access to the information about the top quark spin, and allows to study the top-antitop quark spin correlations in the top pair production. There are two weak decays in succession:  $t \rightarrow Wb$ , followed by  $W \rightarrow e\bar{\nu}_e$

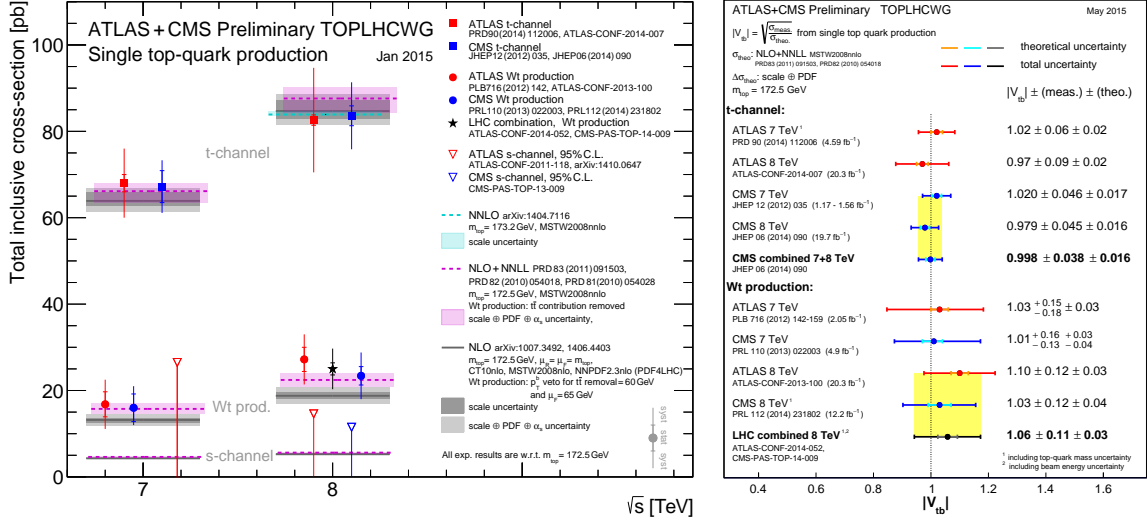


**Figure 6:** Left: A summary of the ATLAS and CMS single top cross section measurements in the  $t$ ,  $Wt$  channels and the limits on the production in the  $s$  the channel. Right: the corresponding values of  $|V_{tb}|$  in the  $t$  and  $Wt$  channels. References to the original publications are listed in the Figure.

or  $W \rightarrow \mu \bar{\nu}_\mu$ . Both decays violate parity ( $\mathcal{P}$ ). One can infer the spin direction of the top quark by measuring the helicity of a  $W$  from top quark decay. In the limit of the  $b$ -quark being massless, if the  $W^+$  helicity in top quark rest frame is  $-1$  then the top quark spin was antiparallel to the  $W^+$  momentum. If the  $W^+$  helicity in the top quark rest frame is  $0$ , then the top quark spin was parallel to the  $W^+$  momentum, as explained schematically in Figure 8.

Analogously to the top quark decay, the  $V - A$  electroweak coupling of the  $W$  boson to its decay products allows determination of the  $W$  boson spin by analyzing its decay products, the lepton and the neutrino, or quark and antiquark. The "analysing power" (at LO) is  $\alpha = 1$  for leptons and  $d, s$  quarks;  $\alpha = -0.4$  for  $b$  quark and  $\alpha = -0.3$  for  $u$  quark and neutrinos. In the helicity basis,  $\theta_i$  are the angles between the lepton direction in the top quark rest frame and the top quark direction in the  $t\bar{t}$  rest frame; and analogously for the top antiquark. The double differential distribution for the  $t\bar{t}$  production and decay is given by:

$$\frac{1}{\sigma} \frac{d^2\sigma}{d\cos\theta_1 d\cos\theta_2} = \frac{1}{4} (1 + \alpha_1 P_1 \cos\theta_1 + \alpha_2 P_2 \cos\theta_2 - C \cos\theta_1 \cos\theta_2)$$

and the single differential distribution is:

$$\frac{1}{\sigma} \frac{d\sigma}{d\cos\theta_i} = \frac{1}{2} (1 + \alpha_i P_i \cos\theta_i)$$

where  $P_i$  is the top quark polarization, and  $C$  is the  $t\bar{t}$  spin correlation.

$$C = \frac{N(\uparrow\uparrow) + N(\downarrow\downarrow) - N(\uparrow\downarrow) - N(\downarrow\uparrow)}{N(\uparrow\uparrow) + N(\downarrow\downarrow) + N(\uparrow\downarrow) + N(\downarrow\uparrow)}$$

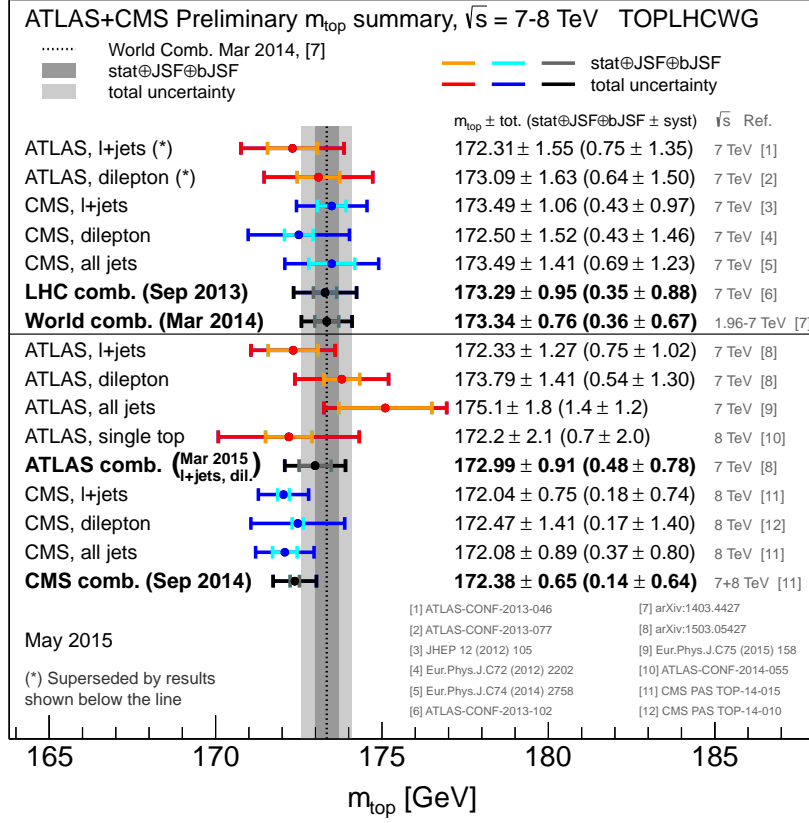


**Figure 7:** A summary of the ATLAS, CMS and the LHC and world combinations of the top quark direct mass measurements. References to the original publications are listed in the Figure.

The longitudinal polarization is parity-odd ( $\mathcal{P}$ -odd); if  $\hat{p}$  is a unit vector in the top momentum direction and  $\vec{S}$  is the top quark spin

$$P_L = \langle \vec{S} \cdot \hat{p} \rangle$$

$$\mathcal{P}(P_L) = -P_L$$

The transverse polarization is parity-even. If  $(\hat{p} \times \hat{k}) = \hat{n}$  is a unit vector perpendicular to the reaction plane, and  $\hat{k}_t$  ( $\hat{k}_{\bar{t}}$ ) is the unit vector in the top quark (top antiquark) momentum direction in the  $t\bar{t}$  centre-of-momentum (cms) frame,

$$P_T = \langle \vec{S} \cdot (\hat{p} \times \hat{k}_t) \rangle$$

$$\mathcal{P}(P_T) = P_T$$

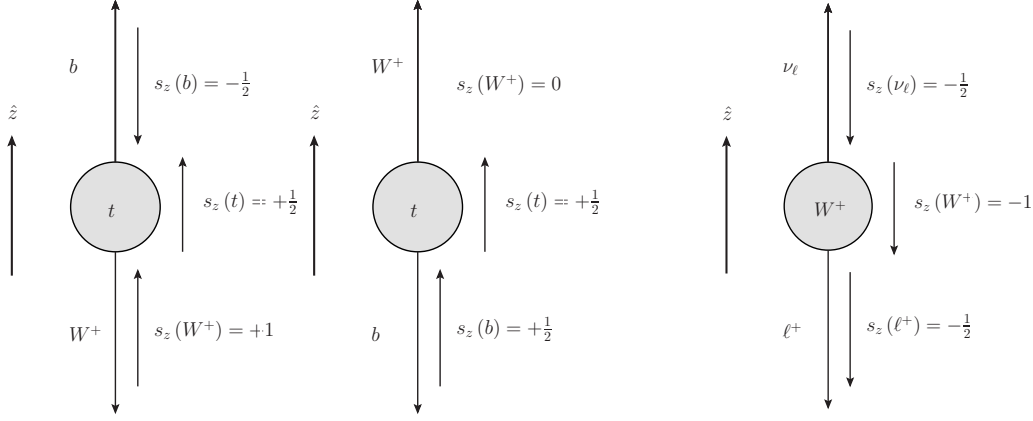


**Figure 8:** Left: Helicity analysis of the top quark decay  $t \rightarrow W^+ b$  decay. Right: Analogous analysis in the subsequent  $W^+ \rightarrow e^+ \nu_e$  decay. One can infer the information about the spin of the parent top quark from analyzing the b-quarks, or leptons from the  $W^+$  decay. An analogous analysis applies to the  $\bar{t} \rightarrow W^- \bar{b}$  decay followed by  $W^- \rightarrow e^- \bar{\nu}_e$  decay

If  $\hat{l}$  is the direction of the lepton momentum in the  $t\bar{t}$  cms frame, then with  $O_T$  defined as:

$$O_T = \text{sign}(\hat{p} \cdot \hat{k}_t)(\hat{n} \cdot \hat{l}^+)$$

or

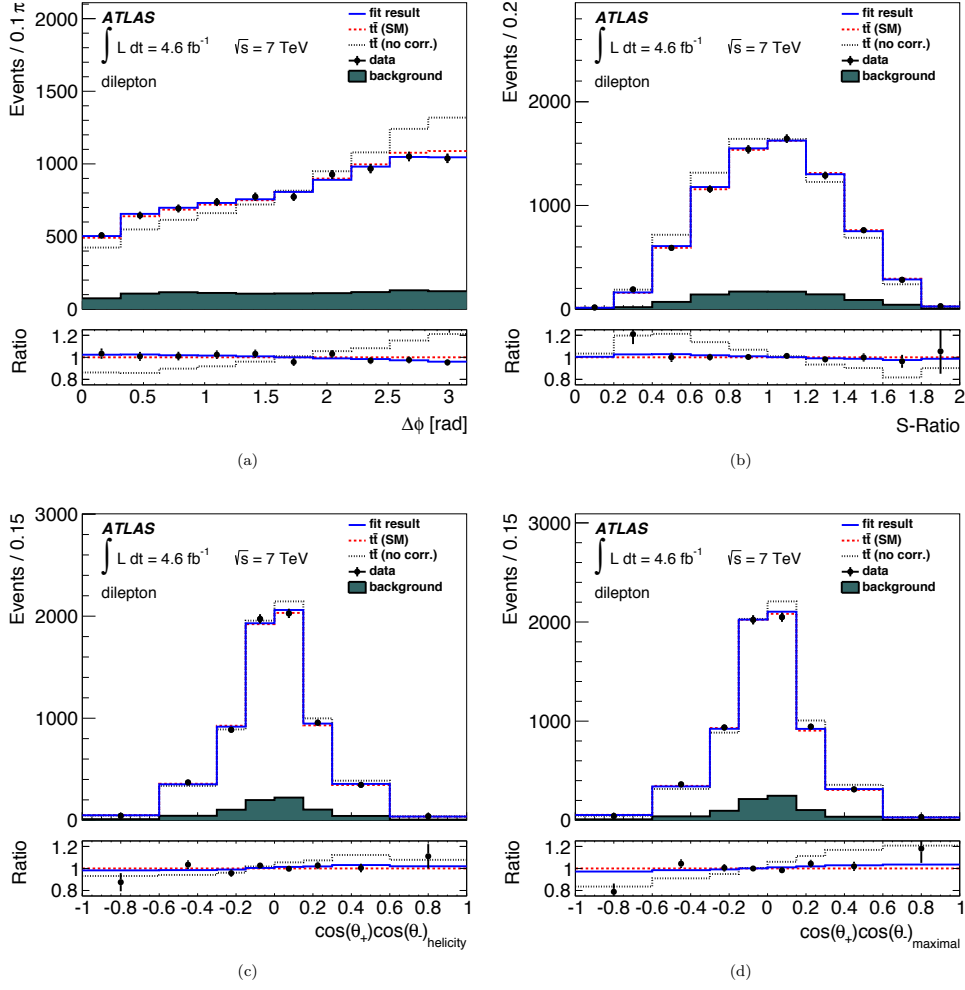
$$O_T = -\text{sign}(\hat{p} \cdot \hat{k}_{\bar{t}})(\hat{n} \cdot \hat{l}^-)$$

$$P_T = \frac{N(O_T > 0) - N(O_T < 0)}{N(O_T > 0) + N(O_T < 0)}$$

The longitudinal polarization is completely unaffected by the transverse polarization in the  $t\bar{t}$  production. The definitions of various asymmetries depend on the choice of observables with which to measure  $P_T$  or  $P_L$ . One can also define variables which are easier to measure experimentally - difference in the azimuthal angle between the top and anti top quarks,  $\Delta\phi_{t\bar{t}}$ , or just the difference in the azimuthal angle between the leptons from the  $W$  decays,  $\Delta\phi_{ll}$ . However, the price for simplicity is that the information about the spin correlations is diluted.

$$A_\phi = \frac{N_{ll}(\cos\phi > 0) - N_{ll}(\cos\phi < 0)}{N_{ll}(\cos\phi > 0) + N_{ll}(\cos\phi < 0)}$$

The ATLAS measurements of top spin correlations[9], based on the  $\sqrt{s} = 7 \text{ TeV}$  di-lepton and lepton+jets data, are summarized in Figure 9. The analysis was performed using four different observables sensitive to different types of "new physics" in  $t\bar{t}$  production, including angular correlations between the charged leptons in two different spin quantization bases, as well as a simple  $\Delta\phi$  between the leptons from the  $W$  decays. The results are presented as measurements of the Standard Model spin correlation fraction,  $f_{SM} = (N_{SM} + N_{uncorrelated})/N_{SM}$ . The results from an analysis of the lepton+jets events, based on  $\sqrt{s} = 8 \text{ TeV}$  data[10] is presented in Figure 10. This measurement has also been used to set lower limits on the mass of the supersymmetric partner of the top quark,  $M_{stop} > 191 \text{ GeV}$  (@95%C.L.). A summary of the D0, CMS and ATLAS measurements of  $f_{SM}$  is shown in the same figure.



Channel	$f_{SM}(\Delta\phi(\ell, \ell))$	$f_{SM}(S\text{-ratio})$	$f_{SM}(\cos(\theta_+) \cos(\theta_-)_{\text{helicity}})$	$f_{SM}(\cos(\theta_+) \cos(\theta_-)_{\text{maximal}})$
$e^+e^-$	$0.87 \pm 0.35 \pm 0.50$	$0.81 \pm 0.35 \pm 0.40$	$1.72 \pm 0.57 \pm 0.75$	$0.48 \pm 0.41 \pm 0.52$
$e^\pm\mu^\mp$	$1.24 \pm 0.11 \pm 0.13$	$0.95 \pm 0.12 \pm 0.13$	$0.76 \pm 0.23 \pm 0.25$	$0.86 \pm 0.16 \pm 0.20$
$\mu^+\mu^-$	$1.11 \pm 0.20 \pm 0.22$	$0.53 \pm 0.26 \pm 0.39$	$0.31 \pm 0.42 \pm 0.58$	$0.97 \pm 0.33 \pm 0.44$
Dilepton	$1.19 \pm 0.09 \pm 0.18$	$0.87 \pm 0.11 \pm 0.14$	$0.75 \pm 0.19 \pm 0.23$	$0.83 \pm 0.14 \pm 0.18$

**Figure 9:** ATLAS top spin correlation results based on an analysis of the dilepton events from  $pp$  collisions at 7 TeV.

## 7. Top asymmetries

At the Tevatron, a  $p\bar{p}$  collider where  $q\bar{q}$  fusion is the dominant  $t\bar{t}$  production process, top quarks tend to follow the proton direction, and top antiquarks the antiproton direction.

There is no forward-backward asymmetry in the  $t\bar{t}$  production in the LO Standard Model calculations, and a very small asymmetry,  $A_{FB-THEORY} = 0.05 \pm 0.015$ , appears only as a result of the interference between the higher order diagrams (NLO): i) interference between the LO and the box diagrams gives rise to a positive  $A_{FB}$ ; ii) interference between the gluon initial and final state

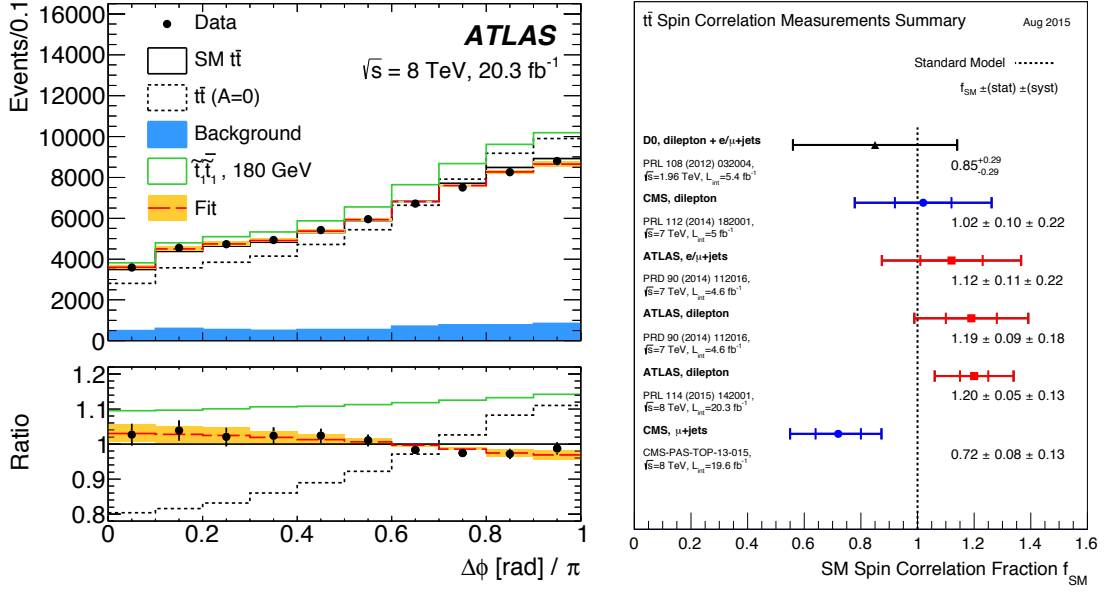


**Figure 10:** Left: ATLAS top spin correlation results based on an analysis of the lepton+jets events from  $pp$  collisions at 8 TeV. Right: A summary of the D0, ATLAS and CMS  $t\bar{t}$  spin correlation measurements. References to the original publications are listed in the Figure.

radiation, which gives rise to a negative  $A_{FB}$ . The Feynman diagrams of the QCD and electroweak corrections to the LO  $t\bar{t}$  production are shown in Figure 11.

CDF measured a larger asymmetry. Based on the data corresponding to the integrated luminosity of 5.3/fb, the combined lepton+jets and di-lepton result was:  $A_{FB} = 0.20 \pm 0.07(\text{stat}) \pm 0.02(\text{sys})$ . This discrepancy created a significant amount of interest for a number of years, and stirred a lot of activity in the field of spin correlations and various asymmetries. Models with heavy bosons  $W', Z'$ , axigluons are a few examples of possible ways to enhance the forward-backward asymmetry by physics beyond the SM, which have been proposed as possible explanation for the CDF result. However, with the more complete results available, both from experiment and theoretical calculations, the discrepancy may be fading away. The higher order (NNLO)  $t\bar{t}$  production calculations by Czakon and Mitov basically agree[12] now with the D0 measurement and differ only by  $\sim 1.7\sigma$  from the final CDF results, based on 9.7/fb, as shown in the top part of Figure 12.

At the LHC, a proton-proton machine, the  $t\bar{t}$  production is, as a consequence of charge conjugation symmetry, forward-backward symmetric in the laboratory reference frame. However, by appropriately selecting the invariant mass of the  $t\bar{t}$  +gluon system and its longitudinal momentum, or the rapidity of the top (antitop) quark, one can constrain the kinematical region in order to generate a preferred direction for quark-antiquark reactions. In this way one can enhance the contribution from the  $q\bar{q}$ ,  $gq$  and  $g\bar{q}$  processes which may give rise to asymmetry, while the  $gg$  process does not contribute to asymmetry. A comparison of the rapidity distributions for top quarks and top antiquarks[11], is sketched in Figure 12, for the Tevatron ( $p\bar{p}$ ) and the LHC ( $pp$ ) accelerators.

At the LHC, these asymmetries are called "charge" symmetries, while at the Tevatron "forward-backward" asymmetries. At the Tevatron, the charge asymmetry is equivalent to the forward-

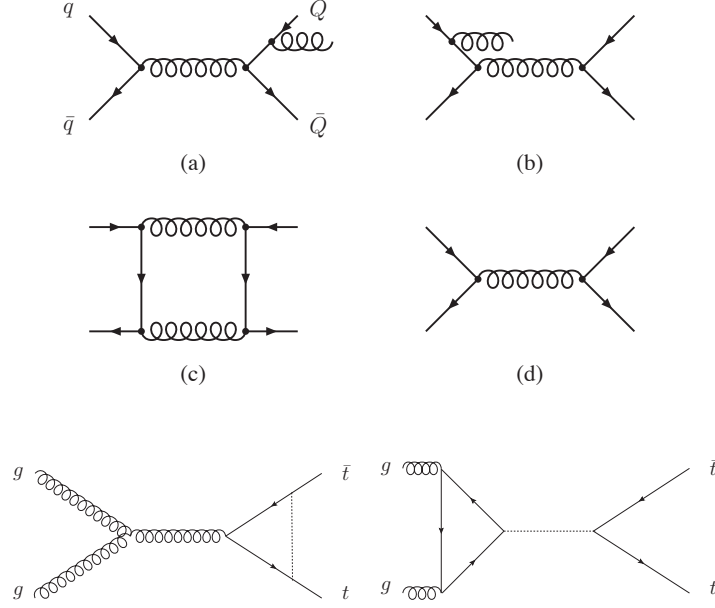


**Figure 11:** NLO corrections to the  $t\bar{t}$  production resulting in the forward-backward asymmetry: Top: QCD corrections - interference between the gluon initial and final state radiation diagrams (a) and (b); and the interference between the box and and the LO diagram (c) and (d). Bottom: the electroweak NLO corrections to the strong interaction  $t\bar{t}$  production.

backward asymmetry. To measure either asymmetry in the laboratory frame, one has to reconstruct the top or anti-top rapidity,  $y$ .

$$A_{LAB} = \frac{N(y_t > 0) - N(y_t < 0)}{N(y_t > 0) + N(y_t < 0)} = \frac{N(y_t > 0) - N(y_{\bar{t}} > 0)}{N(y_{t\bar{t}} > 0) + N(y_{\bar{t}} > 0)}$$

If it is possible to measure both rapidities simultaneously, one can define the variable  $\Delta y = y_t - y_{\bar{t}}$ . The asymmetry in this variable,  $A_{t\bar{t}}$ , is invariant under Lorentz transformations and is equivalent to the charge asymmetry in the  $t\bar{t}$  rest frame, however, the magnitude of  $A_{t\bar{t}}$  is  $\sim 50\%$  larger than  $A_{LAB}$ , as there is no additional deterioration of the signal due to Lorentz boosts from the  $t\bar{t}$  rest frame to the laboratory system.

$$A_{t\bar{t}} = \frac{N(\Delta y > 0) - N(\Delta y < 0)}{N(\Delta y > 0) + N(\Delta y < 0)}$$

At the LHC, the forward-backward asymmetry vanishes, and instead a charge asymmetry is defined, using  $\Delta|y| = |y_t| - |y_{\bar{t}}|$ , as:

$$A_C^y = \frac{N(\Delta|y| > 0) - N(\Delta|y| < 0)}{N(\Delta|y| > 0) + N(\Delta|y| < 0)}$$

It is possible to define a universal asymmetry[11], measured with respect to the average rapidity,  $Y = (y_t + y_{\bar{t}})/2$ . This universal charge asymmetry is calculated analogously to  $A_{t\bar{t}}$  as a function

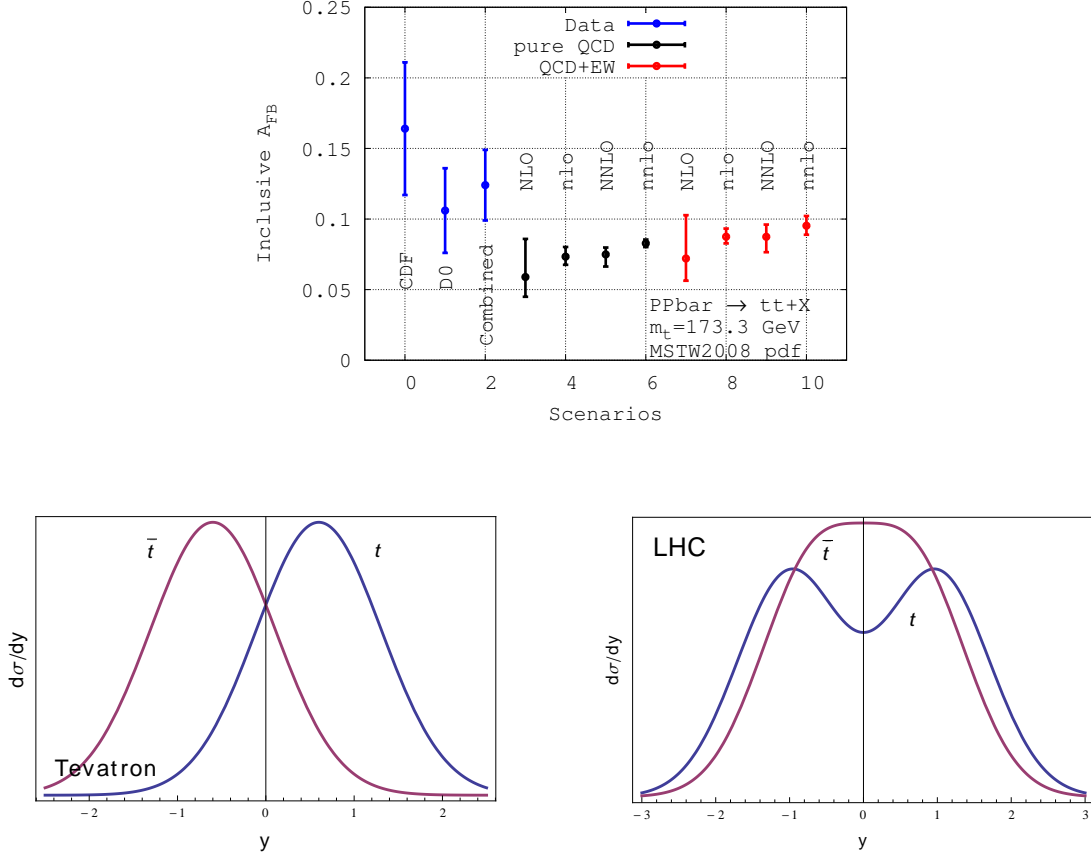
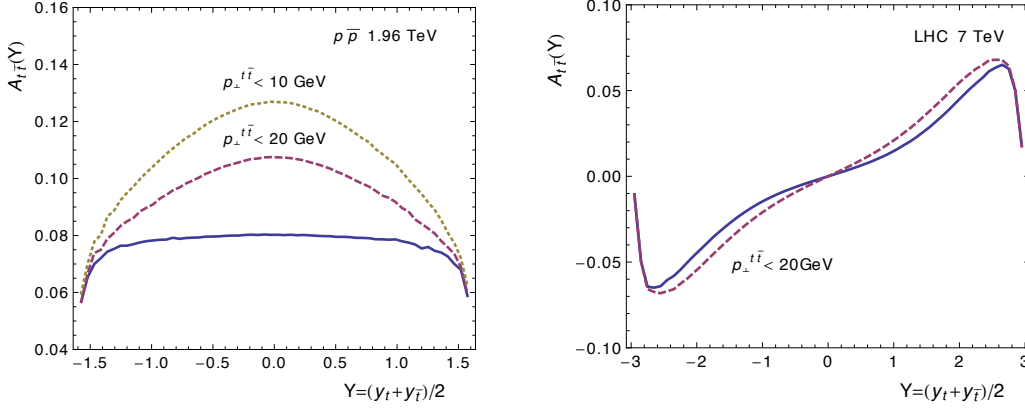


**Figure 12:** Top: The status of NNLO calculations of the forward-backward asymmetry in the  $t\bar{t}$  events and the experimental results from the CDF and D0 experiments at the Tevatron. Bottom: The rapidity distributions of top quark and antiquarks at the Tevatron and the LHC.

of  $Y$ , for events with selected with a definite value of  $Y$ .

$$A_{t\bar{t}}(Y) = \frac{N(\Delta y > 0) - N(\Delta y < 0)}{N(\Delta y > 0) + N(\Delta y < 0)}$$

For the LHC, the universal asymmetry can be enhanced by requiring  $Y > Y_{cut}$ , which suppressed the symmetric  $gg$  and enhances the  $q\bar{q}$  contributions. With the large statistics of  $t\bar{t}$  events at the LHC, such analyses will be pursued by both CMS and ATLAS. The expected  $A_{t\bar{t}}(Y)$  for Tevatron and LHC at 7 TeV are shown in Figure 13, together with a table showing the effect of requiring  $Y > Y_{cut}$ . The  $t\bar{t}$  charge asymmetries are decreasing with increasing LHC  $pp$  collision energy. A summary of the experimental results and theoretical predictions (NLO) is presented in Figure 14. A study by ATLAS[13] examined a number of beyond SM ideas developed to explain the CDF puzzling  $A_{FB}$  result. Figure 15 shows a summary of predictions, together with the experimental bounds as of 2012. (We note that the latest CDF result, based on the full dataset, is in much better agreement with the recent NNLO calculations.)



	$A_C^y$	$A_{t\bar{t}}^{\text{cut}}(Y_{\text{cut}} = 0.7)$
LHC 7 TeV	0.0115 (6)	0.0203 (8)
LHC 8 TeV	0.0102 (5)	0.0178 (6)
LHC 14 TeV	0.0059 (3)	0.0100 (4)
LHC 7 TeV CMS <sup>22</sup>	$0.004 \pm 0.010 \pm 0.012$	
LHC 7 TeV ATLAS <sup>25</sup>	$-0.018 \pm 0.028 \pm 0.023$	

**Figure 13:** Top: The expected distributions of  $A_{t\bar{t}}(Y)$  for Tevatron and LHC at 7 TeV. Bottom: Predicted values of charge asymmetries at different energies of  $pp$  collisions at the LHC. Effects of imposing a requirements  $Y > Y_{\text{cut}}$  are also shown.

## 8. Top exotics

A number searches for a possible structure in the  $t\bar{t}$  mass distribution[14] and in the mass of  $t\bar{t}W$ ,  $t\bar{t}Z$  or  $t\bar{t}\gamma$  systems[15] were performed in ATLAS. A negative search for the  $t\bar{t}$  resonance can be reinterpreted as an exclusion of the Kaluza-Klein gluon in the range  $0.4 - 2.2$  TeV. The  $t\bar{t}$  mass distribution is shown in Figure 16, together with results of searches for the  $t\bar{t}W$ ,  $t\bar{t}Z$  events.

An example of a more detailed study, which undoubtedly be performed with both Run 1 and Run 2 data is shown in Figure 17. With the very large statistics of  $t\bar{t}$  events available, a large number of variables can be examined, and their correlations can be studied more thoroughly, leading to a better understanding of the  $t\bar{t}$  production and its modeling with various Monte Carlo generators.

## 9. Future

The LHC Run started in 2015, with the increased  $pp$  collision energy from 8 TeV to 13 TeV. In addition to the top quark and Higgs boson(s) studies, a complete set of comprehensive searches for NMSSM and other "new physics" will be performed. It is possible that, with an increase of the  $pp$  collision energy, a threshold will be crossed above which new, "beyond SM", particles will be observed, as they may be too heavy to have been produced so far. If not, the physicists working with the LHC experiments will have to turn their attention to the precise measurements of: i) the couplings, branching fractions and properties of the Higgs boson; and ii) studies of top quarks

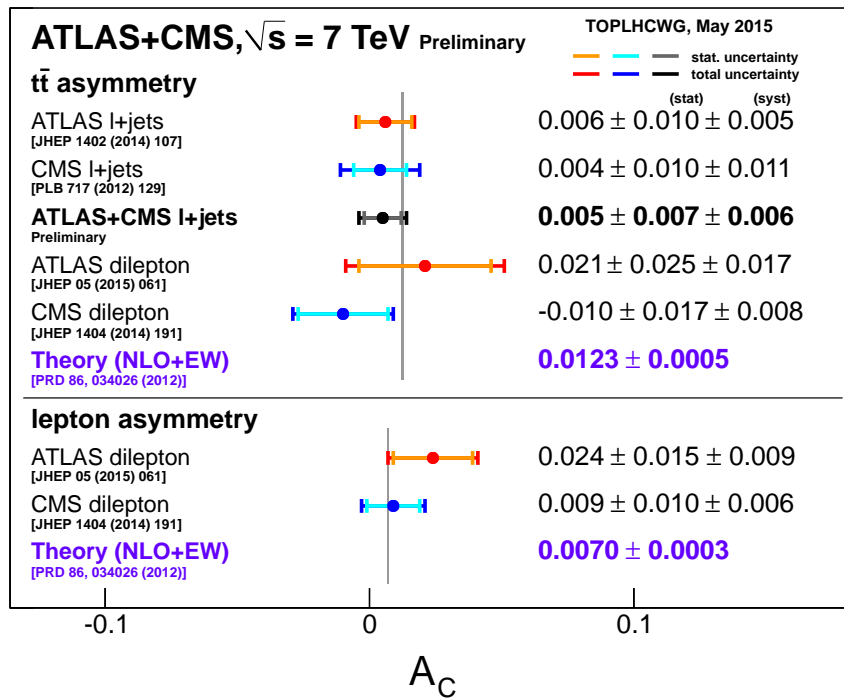


**Figure 14:** A summary of the experimental results and theoretical predictions on the charge asymmetry in  $t\bar{t}$  production. References to the original publications are listed in the Figure.

and spin correlations in  $t\bar{t}$  productions in every possible way. There will be  $\sim 80$  million  $t\bar{t}$  pairs produced in the LHC Run 2.

If no "new physics" is found directly at the LHC in the next few years, the precision studies of the top quark production and decays may be one of the two best windows to study "new physics" indirectly.

## 10. Acknowledgment

I would like to thank the organizers for their warm hospitality and for succeeding in arranging an outstanding workshop, despite encountering many difficulties beyond their control.

## References

- [1] The published ATLAS papers and approved results on the top quark studies can be found at: <https://twiki.cern.ch/twiki/bin/view/AtlasPublic/TopPublicResults>.
- [2] S.L. Glashow, *Partial-symmetries of weak interactions*, Nucl. Phys. **22** (1961) 579; S. Weinberg, *A Model of Leptons*, Phys. Rev. Lett. **19** (1967) 1264; A. Salam, N. Svartholm, ed., *Elementary Particle Physics: Relativistic Groups and Analyticity*, Eighth Nobel Symposium, Stockholm, 1968, Almquist and Wiksell; P.W. Higgs, *Broken Symmetries and the Masses of Gauge Bosons*, Phys. Rev. Lett. **13** (1964) 508; F. Englert, R. Brout, *Broken Symmetry and the Mass of Gauge Vector Mesons*, Phys. Rev. Lett. **13** (1964) 321; G. 't Hooft and M. Veltman, *Regularization and Renormalization of Gauge Fields*, Nucl. Phys. **B44** (1972) 189.

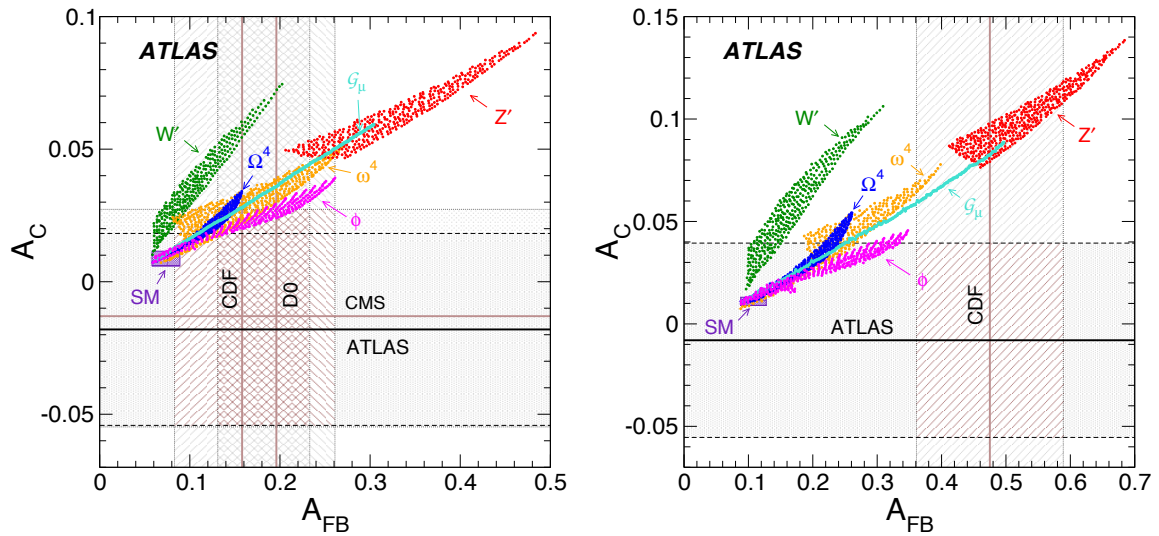


**Figure 15:** Summary of the experimental results and theoretical predictions based on various "beyond the SM" models in which the asymmetries in the  $t\bar{t}$  production could be enhanced. Left: inclusive; Right: with the requirement  $M_{t\bar{t}} > 450 \text{ GeV}$ .

- [3] F. Abe et al., *Evidence for top quark production in  $p\bar{p}$  collisions at  $\sqrt{s} = 1.8 \text{ TeV}$* , Phys. Rev. Lett. **73** (1994) 225
- [4] F. Abe et al., *Observation of Top Quark Production in  $p\bar{p}$  Collisions with the Collider Detector at Fermilab*, Phys. Rev. Lett. **74** (1995) 2626; S. Abachi et al., *Observation of the Top Quark*, Phys. Rev. Lett. **74** (1995) 2632
- [5] Michal Czakon, Paul Fiedler, Alexander Mitov, *The total top quark pair production cross-section at hadron colliders through  $O(\alpha_s^4)$* , Phys. Rev. Lett. **110** (2013) 252004.
- [6] ATLAS Collaboration, *The ATLAS Experiment at the CERN Large Hadron Collider*, JINST **3** (2008) S08003.
- [7] S. Alioli et al., *A new observable to measure the top-quark mass at hadron colliders*, Eur. Phys. J. **C73** (2013) 2438, [arXiv:1303.641]
- [8] ATLAS Collaboration, *Determination of the top-quark pole mass using  $t\bar{t}+1$ -jet events collected with the ATLAS experiment in 7 TeV  $pp$  collisions*, JHEP **10** (2015) 121
- [9] ATLAS Collaboration, *Measurements of spin correlation in top-antitop quark events from proton-proton collisions at  $\sqrt{s} = 7 \text{ TeV}$  using the ATLAS detector*, Phys. Rev. **D90** (2014) 112016
- [10] ATLAS Collaboration, *Measurement of spin correlation in top-antitop quark events and search for stop quark pair production in proton-proton collisions at  $\sqrt{s} = 8 \text{ TeV}$  using the ATLAS detector*, Phys. Rev. Letters **114** (2015) 142001
- [11] G. Rodrigo, *The  $t\bar{t}$  asymmetry in the Standard Model and beyond*, 47th Rencontre de Moriond, Electroweak 2012, LPN12-074, arXiv:1207.0331v1
- [12] M. Czakon, Nuclear and Particle Physics Proceedings 04/2015; 261-262:115-129

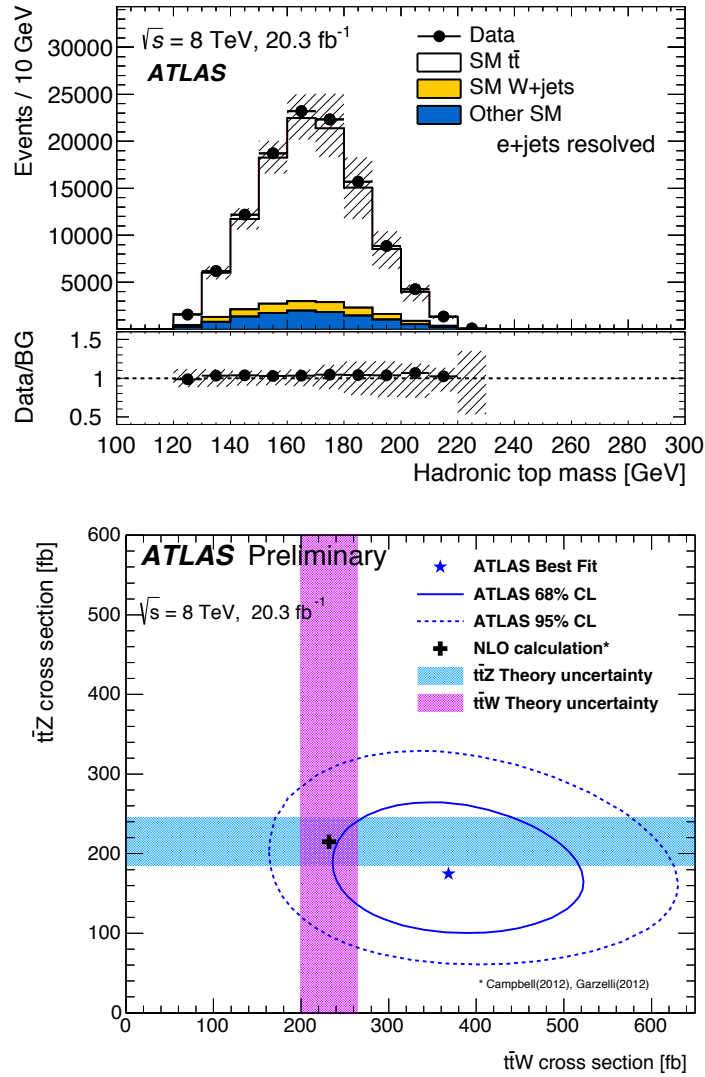


**Figure 16:** Top: The distribution of the  $t\bar{t}$  mass. Bottom: The measurements of the cross sections for  $t\bar{t}W$ ,  $t\bar{t}Z$ , productions, together with the predictions from SM calculations (NLO).

- [13] ATLAS Collaboration, *Measurement of the charge asymmetry in top quark pair production in pp collisions at  $\sqrt{s} = 7$  TeV using the ATLAS detector*, Eur. Phys. J. **C72** (2012) 2039
- [14] ATLAS Collaboration, *A search for  $t\bar{t}$  resonances using lepton plus jets events in proton-proton collisions at  $\sqrt{s} = 8$  TeV with the ATLAS detector*, JHEP 08 (2015) 148, [ATLAS-CONF-2015-009]
- [15] ATLAS Collaboration, *Measurement of the  $t\bar{t}W$  and  $t\bar{t}Z$  production cross sections in pp collisions at  $\sqrt{s} = 8$  TeV with the ATLAS detector*, JHEP11 (2015) 172, [ATLAS-CONF-2015-032]

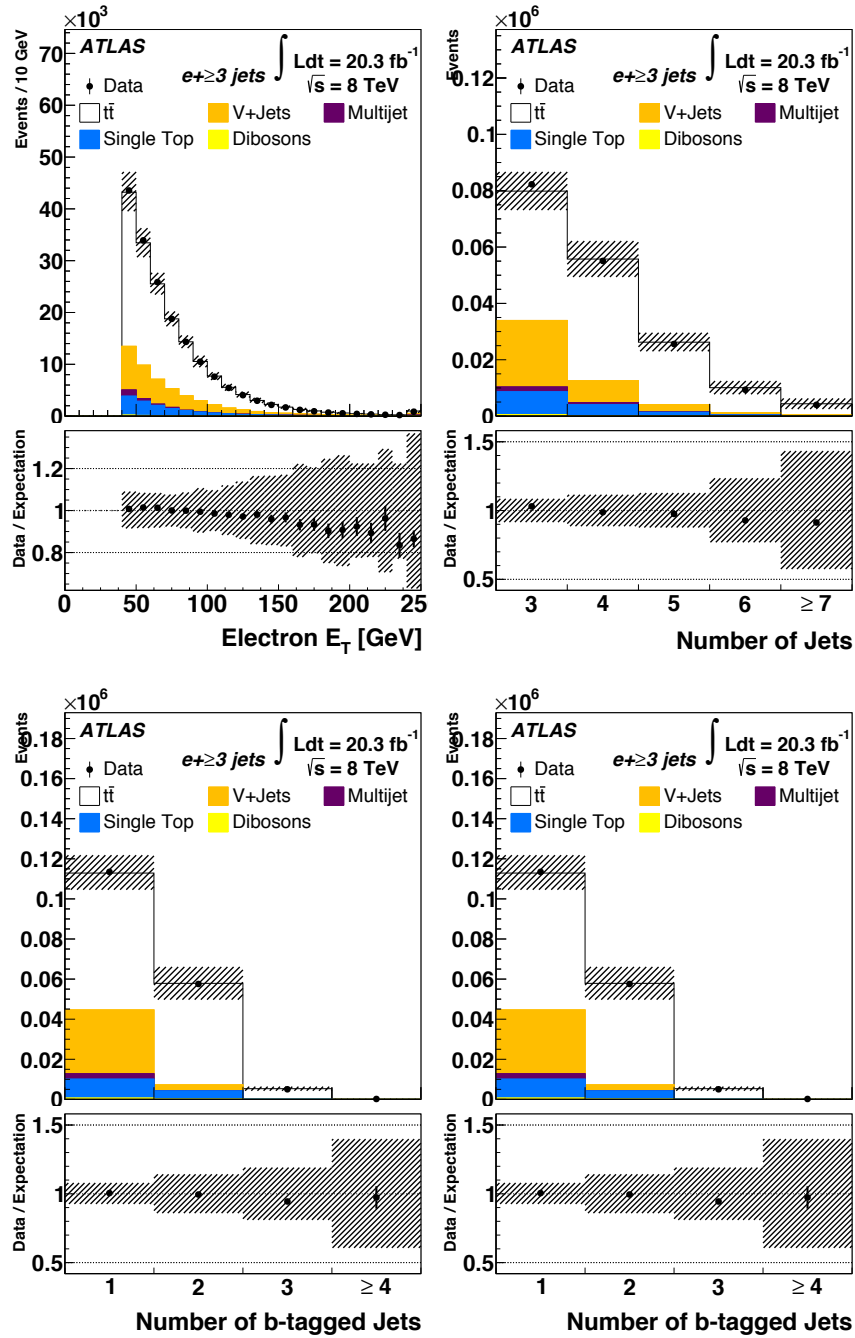


**Figure 17:** Differential distributions of the transverse electron energy, the number of jets, the number of tagged jets and the planarity, based on 20/fb of the 8 TeV data. The same analysis yields the  $t\bar{t}$  cross section  $\sigma_{t\bar{t}} = 260 \pm 1(stat) \pm 23(syst) \pm 8(lum)$  pb.